Check for updates

Coxiella burnetii-containing vacuoles interact with host recycling endosomal proteins Rab11a and Rab35 for vacuolar expansion and bacterial growth

Brooke A. Hall[1], Kristen E. Senior[1], Nicolle T. Ocampo[2]
and Dhritiman Samanta[1*]

[1]Department of Microbiology and Immunology, College of Graduate Studies, Midwestern University,
Glendale, AZ, United States, [2]Arizona College of Osteopathic Medicine, Midwestern University,
Glendale, AZ, United States

Introduction: *Coxiella burnetii* is a gram-negative obligate intracellular bacterium and a zoonotic pathogen that causes human Q fever. The lack of effective antibiotics and a licensed vaccine for *Coxiella* in the U.S. warrants further research into *Coxiella* pathogenesis. Within the host cells, *Coxiella* replicates in an acidic phagolysosome-like vacuole termed *Coxiella*-containing vacuole (CCV). Previously, we have shown that the CCV pH is critical for *Coxiella* survival and that the *Coxiella* Type 4B secretion system regulates CCV pH by inhibiting the host endosomal maturation pathway. However, the trafficking pattern of the 'immature' endosomes in *Coxiella*-infected cells remained unclear.

Methods: We transfected HeLa cells with GFP-tagged Rab proteins and subsequently infected them with mCherry-*Coxiella* to visualize Rab protein localization. Infected cells were immunostained with anti-Rab antibodies to confirm the Rab localization to the CCV, to quantitate Rab11a and Rab35-positive CCVs, and to quantitate total recycling endosome content of infected cells. A dual-hit siRNA mediated knockdown combined with either immunofluorescent assay or an agarose-based colony-forming unit assay were used to measure the effects of Rab11a and Rab35 knockdown on CCV area and *Coxiella* intracellular growth.

Results: The CCV localization screen with host Rab proteins revealed that recycling endosome-associated proteins Rab11a and Rab35 localize to the CCV during infection, suggesting that CCV interacts with host recycling endosomes during maturation. Interestingly, only a subset of CCVs were Rab11a or Rab35-positive at any given time point. Quantitation of Rab11a/Rab35-positive CCVs revealed that while Rab11a interacts with the CCV more at 3 dpi, Rab35 is significantly more prevalent at CCVs at 6 dpi, suggesting that the CCV preferentially interacts with Rab11a and Rab35 depending on the stage of infection. Furthermore, we observed a significant increase in Rab11a and Rab35 fluorescent intensity in *Coxiella*-infected cells compared to mock, suggesting that *Coxiella* increases the recycling endosome content in infected cells. Finally, siRNA-mediated knockdown of Rab11a and Rab35 resulted in significantly

smaller CCVs and reduced *Coxiella* intracellular growth, suggesting that recycling endosomal Rab proteins are essential for CCV expansion and bacterial multiplication.

Discussion: Our data, for the first time, show that the CCV dynamically interacts with host recycling endosomes for *Coxiella* intracellular survival and potentially uncovers novel host cell factors essential for *Coxiella* pathogenesis.

1 Introduction

Coxiella burnetii is a highly infectious, zoonotic, bacterial pathogen and the causative agent of human Q (query) fever. In acute cases, Q fever manifests as a flu-like illness, whereas in about 5% of patients, the disease progresses to a chronic stage that often leads to life-threatening endocarditis (Maurin and Raoult, 1999). The treatment plan for chronic Q fever involves an 18-month-long combined antibiotic therapy and currently, there is no Q fever vaccine licensed in the U.S., presenting challenges in both treating and preventing the disease. Q fever has emerged as a significant public health concern worldwide (Lyytikainen et al., 1998; Amitai et al., 2010; Porter et al., 2011; Nett et al., 2013; White et al., 2013; Angelakis et al., 2014; Bjork et al., 2014; Eldin et al., 2014; Alonso et al., 2015).

In the course of a natural infection, *Coxiella* is transmitted through the respiratory route, where alveolar macrophages within the lung parenchyma endocytose the bacteria (Graham et al., 2016; Dragan et al., 2019). Following entry into host cells, *Coxiella* resides in a tight-fitting phagosome that expands and matures over the next 48–72 hours by interacting with the host endocytic pathway (Howe and Mallavia, 2000). The phagosome maturation pathway involves sequential fusion with the host early and late endosomes, incorporating their respective membrane markers Rab5 and Rab7 (Howe and Mallavia, 2000; Voth and Heinzen, 2007) and subsequent fusion with lysosomes, acquiring lysosomal markers such as LAMP1 (lysosome-associated membrane glycoprotein-1) and vacuolar ATPase (Horwitz, 1983; Clemens and Horwitz, 1995; Huang et al., 2010; Connor et al., 2015; Magunda et al., 2016). The phagosome-lysosome fusion is a unique event in the *Coxiella* life cycle that generates an acidic phagolysosome-like vacuole with a pH of ~5.2 (Mulye et al., 2017; Samanta et al., 2019), within which the bacteria multiply. The mature phagosome, termed the *Coxiella*-containing vacuole (CCV), is crucial to *Coxiella* metabolism, replication, and pathogenesis (Voth and Heinzen, 2007; Ghigo et al., 2012; Newton et al., 2013).

Previously, using a ratiometric fluorescence-based pH measurement assay, we demonstrated that although the CCV is acidic, further escalation in CCV acidity is bactericidal to *Coxiella*

(Mulye et al., 2017) and therefore, *Coxiella* actively regulates CCV acidity in a type 4B secretion system (T4BSS)-dependent manner (Samanta et al., 2019). Specifically, we showed that *Coxiella* T4BSS inhibits the host endosomal maturation pathway, markedly reducing the number of acidic, mature endosomes and lysosomes available for fusion with the CCV (Samanta et al., 2019). Since the CCV attains its luminal acidity by fusing with mature endosomes and lysosomes, inhibiting endosomal maturation indirectly aids *Coxiella* in regulating the CCV pH (Samanta et al., 2019). One notable outcome of *Coxiella* inhibition of endosomal maturation is the increase in mean endosomal pH (pH ~5.2) in the infected cells. Since mature endosomes have a significantly lower pH (~ 4.7), we define the endosomes with an elevated pH as 'immature' endosomes. Because endosomal maturation is crucial to cargo transport and degradation (Huotari and Helenius, 2011), the 'immature' endosomes in *Coxiella*-infected cells may be impaired in these functions and therefore detrimental to host cells. However, the fate and the trafficking pattern of the 'immature' endosomes in *Coxiella*-infected cells remained unclear. In this study, we aim to characterize the endosomal trafficking in *Coxiella*-infected cells by using HeLa cells expressing endosome-specific fluorescent markers analyzed by quantitative confocal microscopy.

The Ras-associated binding (Rab) proteins are the largest family in the Ras superfamily GTPases and are the master regulators of all vesicular trafficking in mammalian cells (Wandinger-Ness and Zerial, 2014). Rab proteins localize on the cytosolic surface of endosomes and perform functions like cargo selection and sorting, vesicle transport along microtubules, and vesicle tethering and fusion with target organelles (Wandinger-Ness and Zerial, 2014). The human genome encodes more than 60 Rab proteins that are associated with specific endosome populations to regulate their trafficking, sorting, and recycling events. Rab proteins cycle between an active, GTP-bound, membrane-recruited form and an inactive, GDP-bound, cytosolic form to associate and dissociate with specific endosomes (Huotari and Helenius, 2011; Wandinger-Ness and Zerial, 2014). Therefore, the localization of a specific Rab protein provides key information about the trafficking pattern of a population of endosomes in mammalian cells.

To understand the trafficking of the *Coxiella*-generated 'immature' endosomes, we ectopically expressed EGFP-tagged Rab proteins in the infected host cells and analyzed their localization by confocal microscopy. To our surprise, we observed that the CCV, in addition to acquiring late endosomal and lysosomal markers, acquired the recycling endosomal markers Rab11a and Rab35. We also observed an increase in Rab11a and Rab35-positive recycling endosomes in the infected cells, indicating that *Coxiella* enhances the recycling endosome content in the infected cells. Finally, silencing Rab11a and Rab35 using siRNA resulted in significantly smaller CCVs and reduced *Coxiella* intracellular growth, suggesting that recycling endosomes facilitate CCV expansion and *Coxiella* multiplication. Our study is the first report suggesting a CCV-host recycling endosome interaction indicating the importance of recycling endosomes in the *Coxiella* intracellular life cycle.

2 Materials and methods

2.1 Bacteria and mammalian cells

Coxiella burnetii Nine Mile Phase II (NMII) (Clone 4, RSA 439) and mCherry-expressing *C. burnetii* NMII (Beare et al., 2009) were grown and stored as previously described (Samanta et al., 2019). Human cervical epithelial cells (HeLa, ATCC CCL-2) were maintained in Roswell Park Memorial Institute (RPMI) 1640 medium with glutamine (Cat. 10–040-CV, Corning, New York, NY) and 10% fetal bovine serum (FBS; Cat. S11150, R&D Systems, Inc., Minneapolis, MN). The genome equivalents (GE) for the *Coxiella* stocks were determined by qPCR using primers for the *Coxiella burnetii dotA* gene (Coleman et al., 2004). The multiplicities of infection (MOI) of the bacteria stocks were optimized for HeLa cells and each type of culture vessels to ~1 internalized bacterium per cell at 37 °C and 5% CO_2.

2.2 Preparation of EGFP-tagged Rab plasmids

The plasmids encoding EGFP-tagged Rab proteins were generous gifts from Dr. Mary Weber, University of Iowa (Faris et al., 2019). The plasmids were first transformed into competent *E. coli* DH5α (Cat. C2988J, New England Biolabs, Ipswich, MA) and stored at -80˚C. A single colony of the transformed *E. coli* was grown in 5 mL lysogeny broth (LB) containing 50 µg/mL kanamycin or 100 µg/mL carbenicillin overnight, which was then used to inoculate a 150 mL LB culture and incubated overnight. The GeneJET Endo-free Plasmid Maxiprep Kit (Cat. K0861, Thermo Fisher Scientific Baltics UAB, Lithuania) was used to isolate and purify plasmid DNA from bacterial cultures according to the manufacturer's protocol. Plasmids were then concentrated using the MilliporeSigma Amicon Ultra-0.5 Centrifugal Filter Units (Cat. UFC503096, Fisher Scientific, Waltham, MA) and stored at -20˚C until used for cell transfection.

2.3 Transfection and immunofluorescent assay

HeLa cells, grown in RPMI with 10% FBS (hereafter referred to as 10% RPMI), were plated in a 24-well plate ($2x10^4$ cells per well) and simultaneously transfected with 0.4 µg of respective EGFP-Rab plasmids using FuGENE 6 transfection reagent (Cat. E269A, Promega, Madison, WI) per the manufacturer's protocol. At 24 hours post-transfection, the cells were infected with mCherry-*Coxiella* in 250 uL 10% RPMI for 1 h, washed extensively with sterile phosphate-buffered saline (PBS; HyClone, Cat. SH30256.01, Cytiva, Marlborough, MA), and incubated in 10% RPMI at 37˚C. On the day before the indicated time points, cells were trypsinized, counted, and diluted to $1x10^5$ cells/mL. Diluted cells were then plated onto coverslips placed in a separate 24-well plate ($5x10^4$ cells per coverslip) and allowed to adhere overnight. The next day, cells were fixed in 2.5% paraformaldehyde (PFA; Cat. 15710, Electron Microscopy Sciences, Hatfield, PA) for 15 min, washed in PBS, and blocked/permeabilized for 20 min in 1% bovine serum albumin (BSA; Cat. BP9700–100, Fisher BioReagents, Pittsburgh, PA) and 0.1% saponin (Cat. S0019, TCI America, Portland, OR) in PBS. Cells were then incubated in rabbit anti-LAMP1 (1:1000; Cat. PA1–654A, Thermo Fisher Scientific, Waltham, MA) primary antibody for 1h followed by Alexa Fluor secondary antibody (1:1000; Life Technologies) for 1 h to label the CCV. Following washing with PBS, coverslips were mounted using ProLong Gold Antifade Mountant with 4', 6'-diamidino-2 phenylindole (DAPI; Cat. P36941, Invitrogen, Carlsbad, CA) and visualized on a Leica Stellaris confocal microscope using a 63x oil immersion objective. Images were processed and analyzed in ImageJ FIJI (Schindelin et al., 2012).

2.4 Enumeration of Rab11a/Rab35-positive CCVs

HeLa cells were plated at $5x10^4$ cells/well in a 6-well plate and incubated overnight. On the following day, the cells in each well were infected with mCherry-*Coxiella* in 500 µL of 10% RPMI for 1 hour at 37°C, washed with PBS, and incubated in 10% RPMI. On the day before the indicated time points, the infected cells were trypsinized and harvested from the 6-well plate, diluted to $1x10^5$ cells/mL, and plated on coverslips in a 24-well plate ($5x10^4$ cells per coverslip) and incubated overnight. The cells were fixed the following day using 2.5% PFA for 15 min at room temperature. Immunofluorescent assay (IFA) was performed by blocking and permeabilizing the cells for 20 min at room temperature using 1% BSA-PBS with 0.1% saponin. Subsequently, the coverslips were incubated in rabbit anti-Rab11a for 72 h at 4°C (1:100; Cat. 715300, Invitrogen) or rabbit anti-Rab35 for 72 h at 4°C (1:500; Cat. ab152138, Abcam, Waltham, MA). Coverslips were then washed with PBS and incubated in Alexa Fluor 488 goat anti-rabbit (1:1000; Cat. A11034, Invitrogen) for 1 h at room temperature. The coverslips were washed with PBS once more before mounting in ProLong Gold Antifade Mountant with DAPI. The cells were

visualized with a Leica Stellaris confocal microscope using a 63x oil immersion objective. For both 3 dpi and 6 dpi, 50–60 CCVs were inspected for Rab11a or Rab35 localization, and the percentage of Rab11a- and Rab35-positive CCVs was determined. The statistical difference in the percent of Rab11a- and Rab35-positive CCVs at each time-point was determined by Welch's t-test from three independent experiments (N=3).

2.5 Quantification of Rab11a and Rab35 content in *Coxiella*-infected cells

HeLa cells were either mock-infected or infected with mCherry-*Coxiella* in 24-well plates ($2.5x10^4$ cells per well; two wells per condition) for 1 h, washed extensively with PBS, and incubated in 10% RPMI. For 3-day experiments, the cells were trypsinized at 2 dpi, diluted to $1x10^5$ cells/mL, and replated onto coverslips in a new 24-well plate ($5x10^4$ cells per coverslip). At 3 dpi, cells were fixed with 2.5% PFA for 15 min and washed thoroughly with PBS. For 6-day experiments, cells were trypsinized, diluted, and replated first at 3 dpi and again at 5 dpi ($5x10^4$ cells per coverslip). Next day, cells were fixed with 2.5% PFA and washed thoroughly with PBS. For both 3-day and 6-day experiments, following fixation, the cells were blocked/permeabilized with 1% BSA in PBS with 0.1% saponin for 20 min. Cells were then incubated overnight at 4°C in rabbit anti-Rab35 (1:100; Cat. 11329–2-AP, Proteintech, Rosemont, IL) or for 1 h at room temperature (RT) in rabbit anti-Rab11a (1:500; Cat. 20229–1-AP, Proteintech) primary antibody. The coverslips were washed with PBS and then incubated in Alexa Fluor 488 goat anti-rabbit (1:1000; Cat. A11034, Invitrogen) secondary antibody for 1 h at RT. Upon washing with PBS, the coverslips were mounted using ProLong Gold with DAPI. Cells were visualized with a Leica Stellaris confocal microscope using a 63x oil immersion objective. To quantify Rab content from mock and WT-infected cells, identically captured and processed images were imported into ImageJ FIJI and the total fluorescent intensity of Rab11a or Rab35 was measured and normalized to cell area. At least 25 cells were analyzed per condition in each of three independent experiments (N=3). The statistical difference in Rab11a and Rab35 intensities between mock and *Coxiella*-infected cells was measured by Welch's t-test.

2.6 RNA interference and immunoblotting

HeLa cells (10^5 cells per well, 6-well plate) were reverse transfected with 50 nM small-interfering RNA (siRNA) SMARTpools specific for human Rab11a (ON-TARGETplus, Cat. L-004726–00-0005, Dharmacon Inc., Horizon Discovery Ltd., Lafayette, CO), Rab35 (ON-TARGETplus, Cat. L-009781–00-0005, Dharmacon Inc.), or a non-targeting (NT) control (Cat. D-001810–10-05, Dharmacon Inc.) using DharmaFECT-1 transfection reagent (Cat. T-2001–01, Dharmacon Inc.) in RPMI with 5% FBS according to the manufacturer's protocol. At 48 h

post-transfection, cells were infected with mCherry-*Coxiella* for 1 h at 37°C. Following washing with PBS, cells were harvested by trypsinization and subjected to a second round of siRNA transfection in a 24-well plate ($2.5x10^4$ cells per well). On the day before the indicated time points, cells were trypsinized, resuspended to $1x10^5$ cells/mL, and either replated onto coverslips ($2.5x10^4$ cells per coverslip) or into another 24-well plate without coverslips. The next day, the cells on coverslips were fixed with 2.5% PFA and subjected to immunofluorescent assay with rabbit anti-LAMP1 primary and Alexa Fluor 488 secondary antibodies to label the CCVs. Concurrently, mock-infected cells from the second 24-well plate were lysed with RIPA lysis buffer (Cat. 89900, Thermo Fisher) supplemented with HALT protease inhibitor (Cat. 87786, Thermo Fisher) on ice. The soluble fraction from the cell lysates were collected and protein concentrations were determined using the Pierce Rapid Gold BCA kit (Cat. A53226, Thermo Fisher). To confirm Rab11a and Rab35 silencing, 10 μg of total protein for both NT and Rab siRNA-transfected samples were resolved in 4–20% gradient SDS-PAGE (Mini-PROTEAN Gel, Cat. 4561094, Bio-Rad Laboratories, Hercules, CA) and subsequently transferred to a PVDF membrane for immunoblotting (Immun-Blot PVDF Membrane, Cat. 1620174, Bio-Rad). After blocking in Bio-Rad EveryBlot buffer (Cat. 12010020, Bio-Rad) for 5 min, the membranes were then probed separately using rabbit anti-Rab11a (Cat. 20229–1-AP, Proteintech), rabbit anti-Rab35 (Cat. 11329–2-AP, Proteintech), and anti-β-tubulin (BT7R) (HRP-conjugated loading control; Cat. MA5–16308-HRP, Invitrogen) antibodies in 1% BSA in PBS. After washing, the membranes were incubated with horseradish peroxidase-conjugated goat anti-rabbit (1:1000; Cat. 31460, Thermo Fisher) secondary antibody in EveryBlot blocking buffer, and developed using enhanced chemiluminescence (ECL) reagent (Cat. 170–5060, Bio-Rad).

2.7 Measurement of CCV area

HeLa cells were reverse-transfected with NT control, Rab11a, or Rab35-specific siRNAs as described above, and at 48 h post-transfection, were infected with mCherry-*Coxiella* for 1 h. Upon washing with PBS, cells were subjected to a second round of siRNA transfection as described above. On the day before the indicated time points, cells were trypsinized, resuspended to $1x10^5$ cells/mL, and replated onto coverslips ($2.5x10^4$ cells/coverslip). The next day, the coverslips were fixed with 2.5% PFA and cells were immunostained with rabbit anti-LAMP1 primary antibody and Alexa Fluor secondary antibody to label the CCVs. Mounted coverslips were visualized using a Keyence BZ-X710 fluorescent microscope. Images of individual CCVs were captured and processed identically between conditions, and the CCV areas from exported images were measured in ImageJ FIJI. A 20 μm scale bar placed on a representative image for each sample was used for setting the scale in ImageJ. CCV areas were expressed as pixels and plotted using GraphPad Prism. At least 25 CCVs were measured per condition for each of the three independent experiments (N=3). The statistical differences in CCV areas between

non-targeting and Rab11a/Rab35-specific siRNA-transfected cells were measured by Welch's t-test.

2.8 Enumeration of viable *Coxiella* by colony forming unit assay

To quantitate *Coxiella* growth in Rab11a and Rab35 knockdown cells we performed an agarose-ACCM-2 media-based colony forming unit (CFU) assay as described previously (Samanta et al., 2019) HeLa cells were reverse-transfected with NT control, Rab11a, or Rab35-specific siRNAs as described above, and at 48 h post-transfection, were infected with mCherry-*Coxiella* for 1 h. Upon washing with PBS, cells were scraped into 2 mL fresh 10% RPMI. Infected cells were then subjected to a second round of siRNA transfection in a new 24-well plate where 2.5×10^4 cells/well were plated for 3 dpi, and 1.25×10^4 cells/well were plated for 6 dpi time-points. To determine viable *Coxiella* at 0 dpi (day of infection), 500 μL (5×10^4) of infected cells were lysed in sterile water for 5 min. The released bacteria were diluted 1:5 in ACCM-2 and plated in 2-fold serial dilutions onto 0.25% ACCM-2 agarose plates. For day 3 and day 6 time points, first, the spent media from the culture wells were collected and centrifuged at 20,000xg for 10 min to pellet any previously released bacteria, and supernatants were discarded (tube 1). The cell monolayers were then lysed in sterile water for 5 min and the released bacteria were diluted 1:5 in ACCM-2 (tube 2). The contents of tubes 1 and 2 were then mixed and spotted in 10-fold serial dilutions onto 0.25% ACCM-2 agarose plates. The plates were incubated for 6–7 days at 37 °C in 2.5% O_2 and 5% CO_2, and the number of colonies counted to measure bacterial viability. Two independent experiments were performed, each with biological duplicates for each condition, and the bacteria were spotted in triplicate. Bacterial growth was expressed as fold change in CFU over 0 dpi and the statistical difference in fold change between NT, siRab11a, and siRab35 conditions were measured using one-way ANOVA with multiple comparisons for each time point.

2.9 Data analyses

Fluorescent and confocal images were processed and analyzed in ImageJ FIJI software (Schindelin et al., 2012). All statistical analyses were performed using unpaired t-test with Welch's correction (Welch's t-test) using GraphPad Prism (GraphPad, La Jolla, CA). A p-value < 0.05 was considered significant. Data are plotted as mean ± standard error of mean (SEM).

3 Results

3.1 Recycling endosomal markers Rab11a and Rab35 localize to the CCV during infection

We previously observed that *Coxiella* actively regulates CCV acidity by inhibiting host endosomal maturation in a T4BSS-dependent manner (Samanta et al., 2019). However, by impeding endosomal maturation, *Coxiella* gives rise to population of 'immature' endosomes with a higher mean pH compared to mature endosomes. As the immature endosomes may be impaired in cargo trafficking and degradation, they may be detrimental to the host cells. However, whether *Coxiella* manipulates the trafficking of the 'immature' endosomes in the infected cells has not been clear. Since Rab proteins are the master regulators of endocytic trafficking, we hypothesized that *Coxiella* manipulates one or more Rab proteins to modulate endosomal trafficking in the infected cells. To test this, we screened 12 major Rab proteins in *Coxiella*-infected cells for their interaction with the CCV. Plasmids encoding EGFP-tagged Rab proteins (Table 1; a gift from Dr. Mary Weber, University of Iowa) were transfected into HeLa cells followed by infection with mCherry-*Coxiella*. At 3 dpi, the cells were immunostained with LAMP1 primary antibody to label the CCVs. During image analysis, CCVs were considered

TABLE 1 EGFP-tagged Rab proteins used in this study.

Rab proteins	Cellular localization	Membrane traffic function	References	Traffics to CCV
Rab1a	ER, Golgi	ER to Golgi	(Plutner et al., 1991)	No
Rab4a	Early endosome	Protein recycling, transport to PM	(van der Sluijs et al., 1992)	No
Rab6a	Golgi	Endosome to Golgi, intra-Golgi transport	(Goud et al., 1990)	No
Rab7	Late endosomes, lysosomes	Late endosome to lysosome	(Chavrier et al., 1990)	Yes
Rab8	Cell membrane, primary cilia	Exocytosis, TGN to PM	(Huber et al., 1993)	No
Rab9	Late endosomes, Golgi	Endosome to TGN	(Yoshimura et al., 2007)	No
Rab11a	Recycling endosomes, Golgi	TGN/RE to PM	(Ren et al., 1998)	Yes
Rab14	Golgi, early endosomes	TGN/RE to PM	(Junutula et al., 2004)	No
Rab18	Golgi, lipid droplets	Lipid droplet formation	(Dejgaard et al., 2008)	No
Rab33	Golgi	Autophagosome formation	(Zheng et al., 1998)	No
Rab34	Golgi	Intra-Golgi transport	(Wang and Hong, 2002)	No
Rab35	Recycling endosomes, PM	RE to PM	(Kouranti et al., 2006)	Yes

ER, Endoplasmic reticulum; PM, plasma membrane; TGN, Trans-Golgi Network; RE, Recycling endosomes.

positive for Rab trafficking based on the qualitative similarity of Rab proteins and LAMP1 localization at the CCV membrane. EGFP tagged-Rab7 was included as a positive control in the screen as previous reports suggest that Rab7 localizes to the CCV during infection (Beron et al., 2002; Romano et al., 2007). As expected, all CCVs were positive for Rab7 and LAMP1. In addition to that, we interestingly observed that some CCVs were also positive for Rab11a and Rab35 as evidenced by their colocalization with LAMP1 at the CCV membrane (Figure 1). Because ectopic expression may affect protein localization, we confirmed Rab11a and Rab35 localization to CCV using respective antibodies (Figure 2A). Both Rab11a and Rab35 are associated with host recycling endosomes, where they regulate the 'slow' and 'fast' endosomal recycling pathways, respectively (Ullrich et al., 1996; Grant and Donaldson, 2009; Chaineau et al., 2013). Therefore, these data suggest that, in addition to interacting with late endosomes and lysosomes, at least a subset of CCVs also interacts with the host recycling endosomes in both the 'slow' and the 'fast' recycling pathways. A CCV area comparison between the Rab11a/Rab35-positive and the negative CCVs showed no significant difference in areas between the positive and the negative CCVs (data not shown). Moreover, *Coxiella* colonies appeared unaffected by the presence or absence of Rab11a and Rab35 at the CCV. This study is the first report suggesting that the CCV interacts with host recycling endosomes and acquires recycling endosomal markers during maturation.

3.2 CCV-Rab11a and CCV-Rab35 interactions are dynamic and temporally regulated

In our Rab CCV localization screen, we interestingly observed that only a subset of the CCVs were positive for Rab11a or Rab35 at a given time point. This led us to hypothesize that the interaction between the CCV and Rab11a/Rab35 are dynamic in nature. To test this, we quantified the percentage of Rab11a- and Rab35-positive CCVs in a population of infected HeLa cells at 3 and 6 dpi using HeLa cells immunostained with anti-Rab11a and anti-Rab35 antibodies. Our data revealed that at 3 dpi, ~47% of CCVs were positive for Rab11a, whereas only ~28% of CCVs were positive for Rab35 (Figures 2B, C). Interestingly this pattern reversed at 6 dpi, when only ~19% of CCVs were positive for Rab11 and ~57% of CCVs were positive for Rab35 (Figures 2B, C). Together, these data suggest that, while CCVs preferentially interact with the Rab11a-positive endosomes at 3 dpi, at 6 dpi, the preferential interaction shifts towards the Rab35-positive endosomes indicating that Rab11a and Rab35 interactions with the CCV are dynamic and vary depending on the stage of infection.
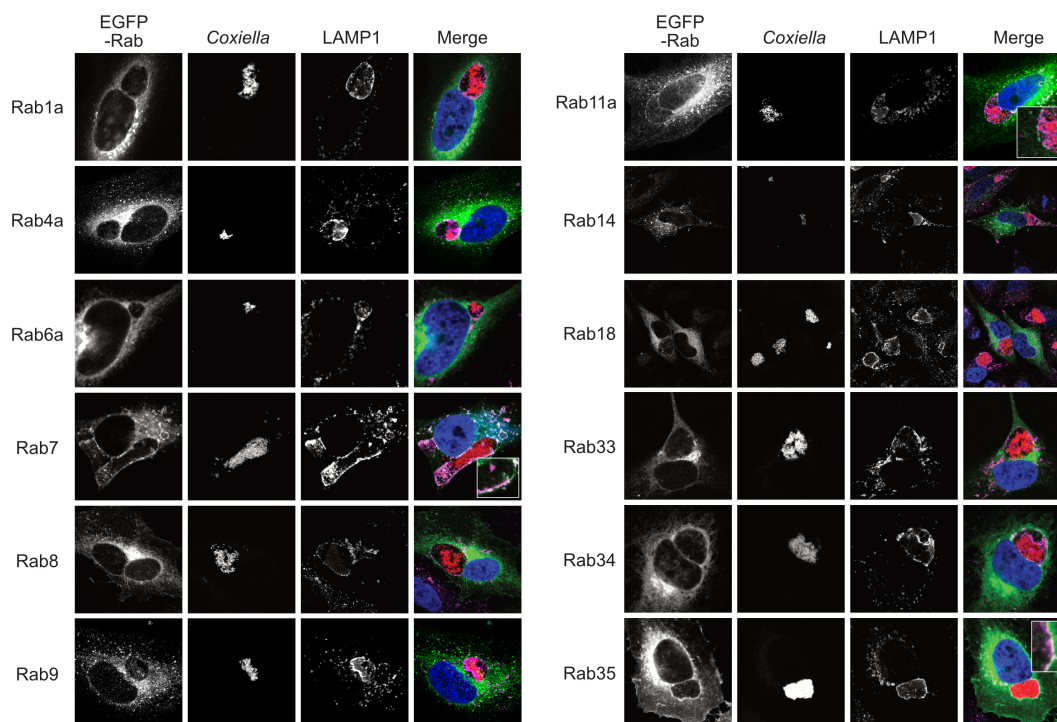

FIGURE 1
Host recycling endosome-associated proteins Rab11a and Rab35 localize to the CCV. Representative images of *Coxiella*-infected HeLa cells, expressing EGFP-tagged Rab proteins. HeLa cells were transfected with plasmids encoding EGFP-Rab proteins and at 24 h post-transfection, were infected with mCherry-*Coxiella* for 1 h. At 3 dpi, cells plated on coverslips were fixed and subjected to immunofluorescent assay with anti–LAMP1 antibody to label the CCVs. Cells were visualized with a Leica Stellaris confocal microscope and images were analyzed in ImageJ FIJI. CCVs, where LAMP1 and Rab proteins colocalized at the membrane (shown in insets) were considered positive for a specific Rab protein. As expected, all CCVs were positive for Rab7 and LAMP1 at 3 dpi. Additionally, we observed that Rab11a and Rab35 also localized to CCVs. Notably, only a subset of CCVs were positive for Rab11a or Rab35.
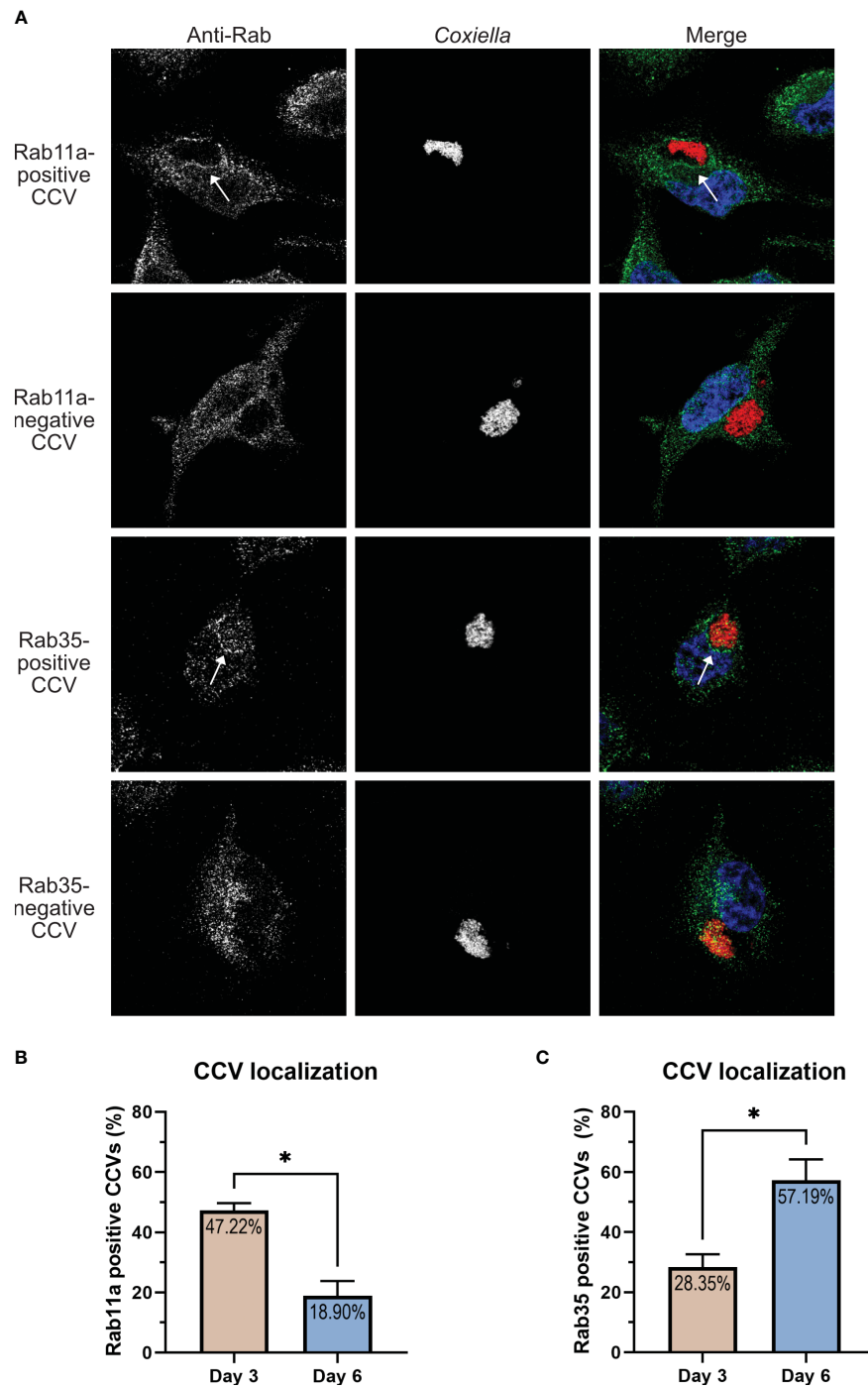
FIGURE 2

CCV-Rab11a and CCV-Rab35 interactions are dynamic and temporally regulated. **(A)** Representative images showing Rab11a and Rab35-positive and negative CCVs. HeLa cells were infected with mCherry *Coxiella* and at 3 dpi, cells plated on coverslips were fixed and subjected to immunofluorescent assay with anti-Rab11a or anti-Rab35 antibodies. Cells were visualized with a Leica Stellaris confocal microscope and CCVs were scored for Rab11a or Rab35 localization and percentage of positive CCVs were calculated. **(B, C)** Quantification of Rab11a- and Rab35-positive and negative CCVs at 3 and 6 dpi revealed that Rab11a localized to significantly more CCVs at 3 dpi compared to 6 dpi, whereas the pattern reversed for Rab35, which localized to more CCVs at 6 dpi. Data shown as mean $\pm$ SEM of 50−60 infected cells per condition in each of three independent experiments (N=3) as analyzed by Welch's t-test; *, P<0.05.

3.3 *Coxiella* infection leads to increased recycling endosome content in infected cells

Our observation that *Coxiella* interacts with two different populations of recycling endosomes in the host cells led to the hypothesis that *Coxiella* manipulates host recycling endosomes during infection. To test this hypothesis, we quantitated the total cellular Rab11a and Rab35 content in mock and *Coxiella*-infected HeLa cells by immunofluorescent assay. Mock and *Coxiella*-infected cells were immunostained using anti-Rab11a or anti-Rab35 antibodies at 3 and 6 dpi and identically captured images were analyzed in ImageJ FIJI. The total fluorescent intensity of Rab11 or Rab35 was measured from mock and *Coxiella*-infected cells normalized to cell area and were considered indicative of total recycling endosome content in each cell. Our data revealed a ~19% increase in Rab11a fluorescent intensity (p < 0.0001; Figures 3A, B) and a ~27% increase in Rab35 fluorescent intensity in infected cells compared to mock at 3 dpi (p < 0.0001; Figures 4A, B). However, interestingly, we did not observe any difference in Rab11a or Rab35 fluorescent intensities between mock and *Coxiella*-infected cells at 6 dpi (Figures 3C, 4C). These data suggest that *Coxiella* increases the recycling endosome content in infected host cells at 3 dpi, but not at 6 dpi.

3.4 Rab11a and Rab35 silencing inhibits CCV expansion and *Coxiella* intracellular growth

Based on our observation that the CCV dynamically interacts with recycling endosome-associated Rab proteins, and that *Coxiella* increases the recycling endosome content of infected cells, we hypothesized that Rab11a and Rab35 positively affects CCV maturation and *Coxiella* intracellular growth. To test this, we first quantified CCV areas in NT control, Rab11a, and Rab35 knockdown HeLa cells using our dual-hit siRNA knockdown protocol (Figure 5A) (Samanta et al., 2019) followed by immunofluorescent assay. Since CCV interaction with Rab11a is higher at 3 dpi, and that with Rab35 is higher at 6 dpi, we measured the CCV areas in Rab11a and Rab35 knockdown cells at 3 and 6 dpi, respectively, to detect maximum effect of the respective knockdowns. Immunoblotting with cell lysates from NT, siRab11a, and siRab35-transfected cells using anti-Rab or anti-β-tubulin antibodies confirmed depletion of both Rab11a (Figure 5B) and Rab35 (Figure 5C) at 3 and 6 dpi, respectively. The CCV area measurement data showed a ~45% reduction in CCV area in Rab11a knockdown cells compared to NT (p<0.0001) at 3 dpi (Figure 6A), and a ~28% reduction in CCV area in Rab35 knockdown cells (p<0.0001) at 6 dpi (Figure 6B) suggesting that both Rab11a and Rab35 positively affect CCV expansion at 3 and 6 dpi, respectively. Next, *Coxiella* growth was quantitated in NT, Rab11a, and Rab35 knockdown HeLa cells by agarose-based CFU assay. Compared to NT, *Coxiella* growth was significantly reduced in both Rab11a and Rab35 knockdown cells at both 3 and 6 dpi (Figure 6C; Table 2). Therefore, these data strongly suggest that host recycling endosomes are essential for CCV expansion and *Coxiella* intracellular growth.

4 Discussion

We previously established that *Coxiella* T4BSS inhibits host endosomal maturation for bacterial survival and pathogenesis. However, in the process, *Coxiella* generates a population of 'immature' endosomes with an elevated mean pH relative to mature endosomes. To comprehensively understand endosomal trafficking in *Coxiella*-infected cells, we screened 12 well-studied Rab proteins to assess their localization in *Coxiella*-infected cells. We discovered that Rab11a and Rab35, the molecular markers of recycling endosomes, localize to the CCV, although only a subset of CCVs were found positive for Rab11a or Rab35 at a given time point. Our data also suggest that *Coxiella* increases the recycling endosome content of the infected cells, and both Rab11a and Rab35 are positive regulators of CCV expansion and *Coxiella* intracellular growth.

Mammalian endosomal trafficking can be broadly classified into degradative and recycling pathways (O'Sullivan and Lindsay, 2020). While the degradative pathway traffics the cargo through early and late endosomes and finally delivers it to lysosomes for degradation, the recycling pathway sorts and re-exports essential membrane components including receptors, carrier molecules, and cell adhesion molecules that have been internalized (Grant and Donaldson, 2009). For the first time, we present findings suggesting an interaction between the CCV and the host recycling endosomes. This intriguing observation implies that the CCV not only engages with the host endocytic degradative endosomes but also with recycling endosomes, potentially incorporating their contents and membranes during maturation. Mammalian cells exhibit two simultaneous pathways for cargo recycling namely the 'fast' and the 'slow' recycling pathways (Hopkins and Trowbridge, 1983). In the 'fast' pathway, the internalized cargo is directly transported back to the plasma membrane from early endosomes whereas the 'slow' pathway traffics cargo to a perinuclear vesicle known as the endocytic recycling compartment (ERC), where the cargo is sorted and then redirected to the plasma membrane via recycling endosomes (Grant and Donaldson, 2009; Allgood and Neunuebel, 2018). Rab35 predominantly regulates the 'fast' recycling pathway (Ullrich et al., 1996; Chaineau et al., 2013), while Rab11a serves as a major regulator of the 'slow' pathway (Ullrich et al., 1996; Green et al., 1997; Grant and Donaldson, 2009). Therefore, our data suggest that the CCV interacts with both the 'fast' and the 'slow' recycling pathways during maturation. Moreover, our observation that Rab11a localizes to the CCVs significantly more at 3 dpi whereas Rab35 is more prevalent at CCVs at 6 dpi suggests a preference for interaction with the 'slow' recycling pathway during the early stages of maturation and a shift towards a preferential interaction with the 'fast' recycling pathway as the CCV matures further. However, elucidating the molecular mechanism of Rab11a and Rab35 recruitment warrants further research. One possibility is that one or more *Coxiella* T4BSS effector proteins recruit Rab proteins to the CCV. Several studies have
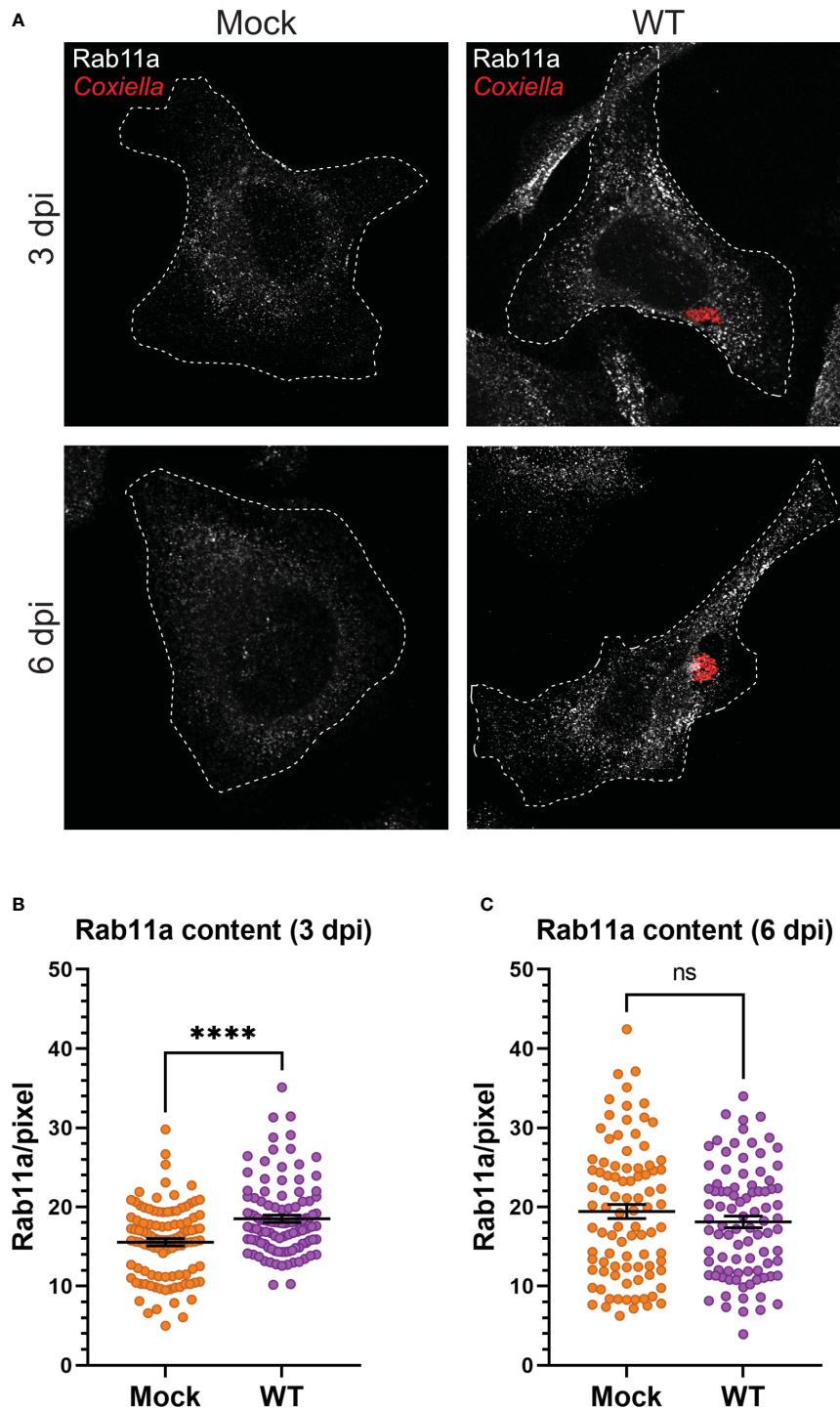
FIGURE 3

Coxiella increases Rab11a content in infected host cells. **(A)** Representative images showing Rab11a-positive recycling endosome content of mock and *Coxiella*-infected HeLa cells at 3 and 6 dpi. HeLa cells were mock infected or infected with mCherry-*Coxiella* for 1 h. On the days before the indicated time points, the cells were plated on coverslips. The next day, cells were fixed and subjected to immunofluorescent assay with anti-Rab11a antibody to uniformly stain the Rab11a-positive recycling endosomes. Cells were visualized with a Leica Stellaris confocal microscope and the images were analyzed in ImageJ FIJI. Identically captured images were imported into ImageJ FIJI and the total fluorescent intensity of Rab11a was measured and normalized to cell area. **(B, C)** Quantification of Rab11a fluorescent intensity revealed an increase in Rab11a content in *Coxiella*-infected cells at 3 dpi but not at 6 dpi. Data shown as mean $\pm$ SEM of at least 25 cells per condition in each of three independent experiments (N=3) as analyzed by Welch's t-test; ****, P<0.0001; ns, non-significant.
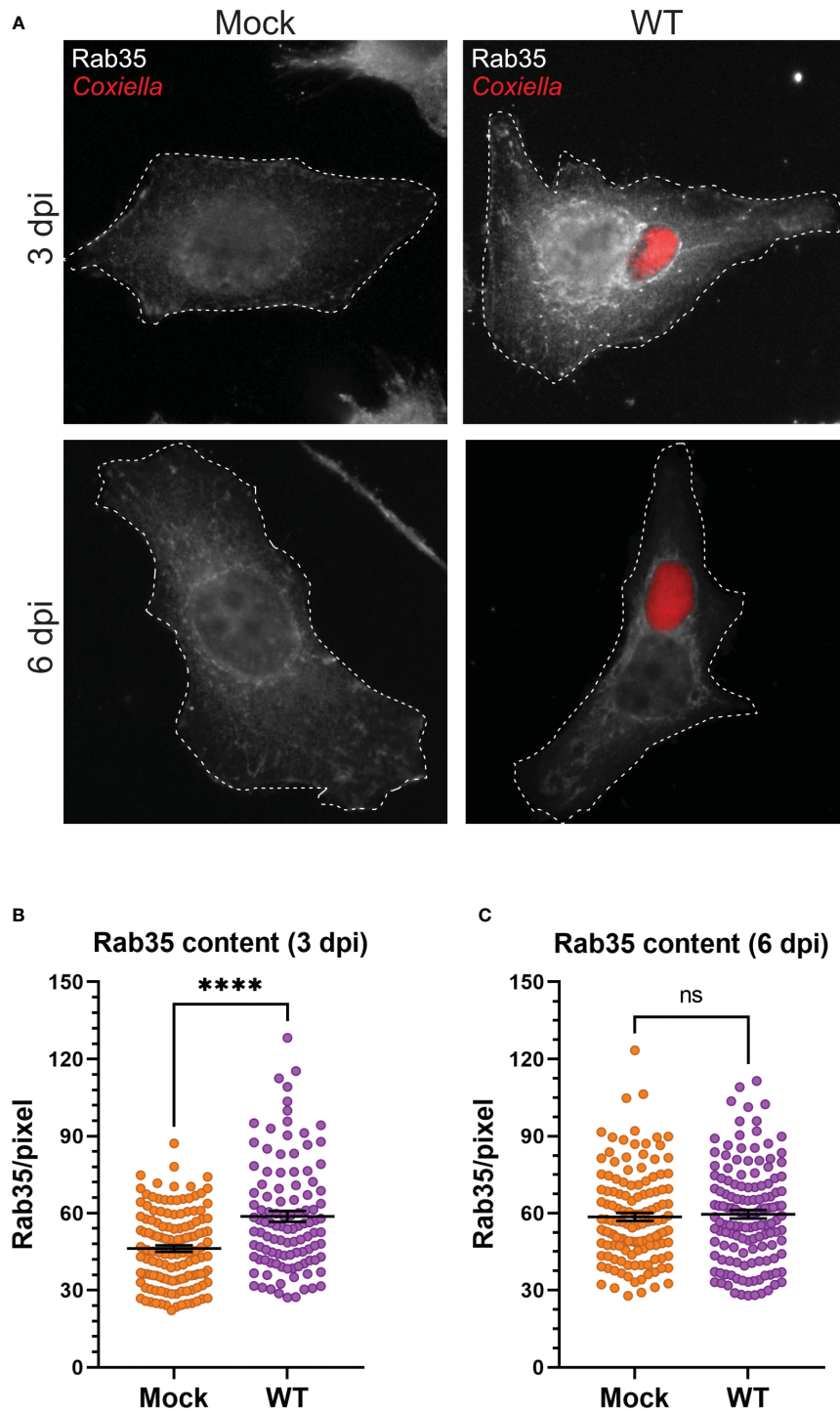
FIGURE 4

Coxiella increases Rab35 content in infected host cells. **(A)** Representative images showing Rab35-positive recycling endosome content of mock and *Coxiella*-infected HeLa cells at 3 and 6 dpi. HeLa cells were mock infected or infected with mCherry-*Coxiella* for 1 h. On the days before the indicated time points, the cells were plated on coverslips. The next day, cells were fixed and subjected to an immunofluorescent assay with anti-Rab35 antibody to uniformly stain the Rab35-positive recycling endosomes. Cells were visualized with a Leica Stellaris confocal microscope and the images were analyzed in ImageJ FIJI. Identically captured images were imported into ImageJ FIJI and the total fluorescent intensity of Rab35 was measured and normalized to cell area. **(B, C)** Quantification of Rab35 fluorescent intensity revealed an increase in Rab35 content in *Coxiella*-infected cells at 3 dpi but not at 6 dpi. Data shown as mean $\pm$ SEM of at least 25 cells per condition in each of three independent experiments (N=3) as analyzed by Welch's t-test; ****, P<0.0001; ns, non-significant.
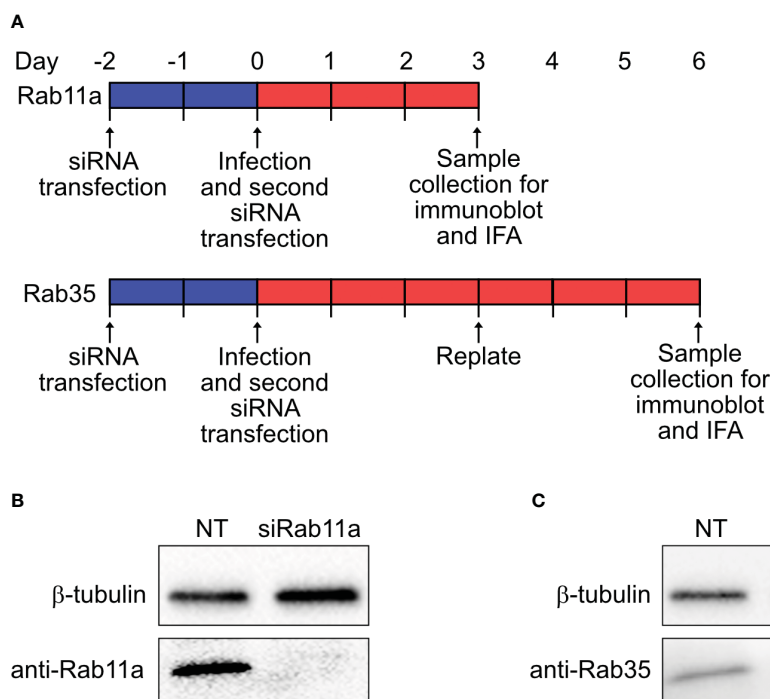
FIGURE 5

Dual-hit gene knockdown successfully depleted Rab11a and Rab35 proteins **(A)** Schematic diagram of dual-hit siRNA transfection protocol in HeLa cells to silence Rab proteins. Cells were transfected with Rab11a or Rab35-specific siRNA or a control non-targeting siRNA (NT) and incubated. At 48 h post-transfection cells were subjected to a second round of siRNA transfection. Cells were immunoblotted at the indicated time points with either an anti-β-tubulin or respective Rab antibodies. **(B, C)** Immunoblots revealed depletion of Rab11a and Rab35 in siRNA-transfected cells at 3 and 6 dpi, respectively.

reported effector proteins' role in interacting with host proteins and/or recruiting them at the CCV (Voth et al., 2009; Kohler et al., 2016; Siadous et al., 2021). This could be an intriguing avenue for future research.

While the significance of the interactions between CCV and the host recycling endosomes remains uncertain, multiple studies propose that similar interactions with intracellular bacterial vacuoles play crucial roles in providing nutrients to the vacuole or in ensuring vacuolar stability. For example, *Chlamydophila pneumoniae*-containing inclusions recruit the mammalian Rab11/Rab14 adapter protein Fip2, facilitating the early-stage recruitment of Rab11/14 to the inclusion membrane during infection (Baetz and Goldenring, 2013; Molleken and Hegemann, 2017). Rab11/14 positive recycling endosomes trafficked nutrients, such as transferrin to the proximity of *C. pneumoniae* inclusion, although whether transferrin is delivered into the inclusion lumen remained unclear (Rejman Lipinski et al., 2009; Ouellette and Carabeo, 2010; Leiva et al., 2013). Indeed, a recent study with fluorescent transferrin (Tf488) revealed that in *Coxiella*-infected HeLa cells, Tf488-containing vesicles also trafficked to the proximity of CCVs (Larson and Heinzen, 2017). Moreover, Rab11-positive recycling endosomes trafficked transferrin in K562 cells (Green et al., 1997). Therefore, it is possible that recycling endosomes traffic transferrin into the CCV aiding in its maturation. Further experimentation is needed to examine this intriguing hypothesis. Another possible benefit of intracellular pathogens subverting recycling endosomes is to augment vacuole stability. For example, *Chlamydia trachomatis*

inclusion protein CT229 interacts with Rab35 to maintain the inclusion integrity (Faris et al., 2019), and *Legionella pneumophila*-containing vacuoles (LCV) acquire Rab11 and Rab35 for stability (Allgood et al., 2017). Therefore, Rab11a and Rab35 may play a critical role in maintaining CCV stability. However, we did not observe a disintegration of CCV in Rab11a and Rab35 knockdown HeLa cells, raising the possibility that *Coxiella* employs redundant mechanisms to maintain CCV stability.

As mentioned before, we observed that only a subset of CCVs are positive for Rab11a or Rab35 at a given time point, and the proportion of Rab11a- and Rab35-positive CCVs in a population of infected cells vary over time. Previous studies, including ours, have only observed stable fusion events between the CCV and host endosomes and lysosomes (Howe et al., 2003; Voth and Heinzen, 2007; Mulye et al., 2017; Samanta et al., 2019). The dynamic nature of CCV-Rab11a/Rab35 interactions could be a result of two possibilities: first, only a subset of CCVs preferentially interacts with the recycling endosomes at a given time point and the number of preferred CCVs interacting with a specific Rab protein varies depending on the stage of infection, and second, it is possible that the recycling endosomes make transient contact with the CCVs in a 'kiss-and-run' manner (Ryan, 2003), to release their content into the CCV and/or to receive recyclable cargo from the CCV and dissociate. However, further experimentation would be required to test these hypotheses, and could be an area of future investigation.

Our observation that *Coxiella* infection led to an increased recycling endosome content at 3 dpi builds upon the previous
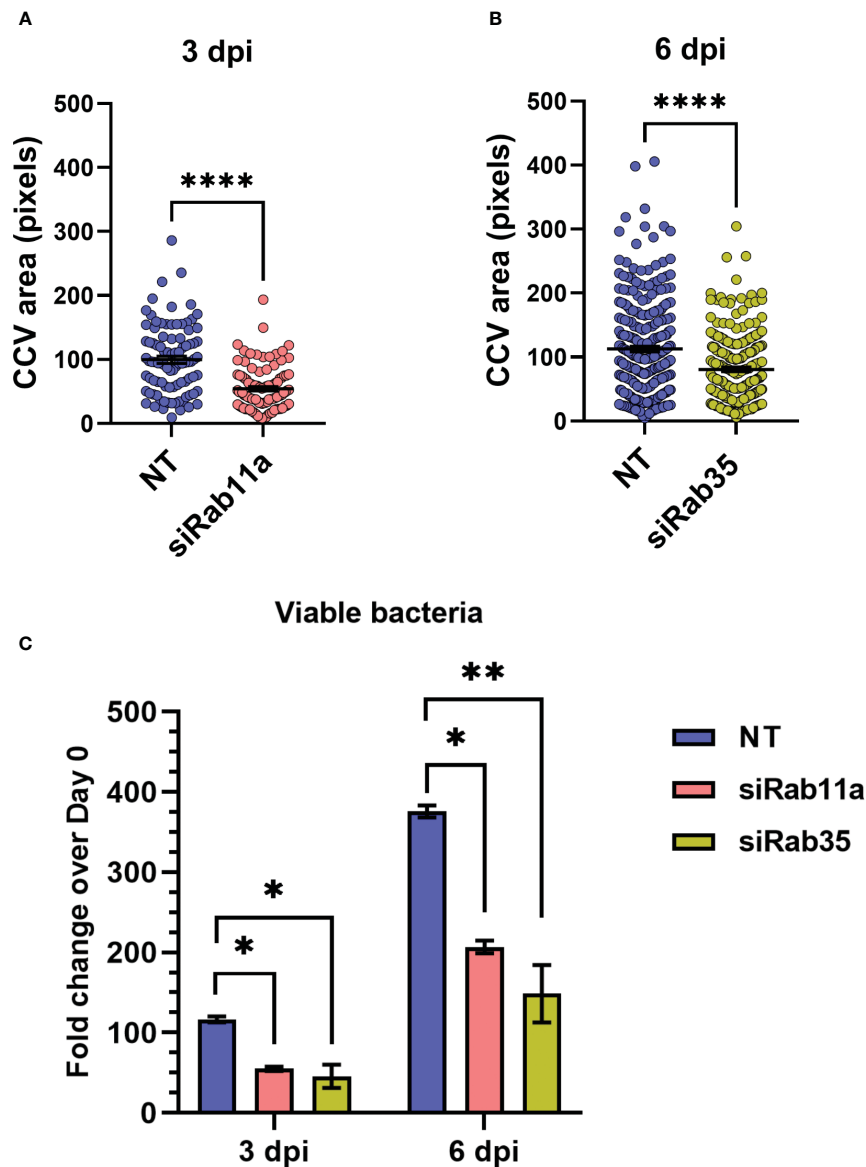
FIGURE 6
Rab11a and Rab35 are essential for CCV expansion and *Coxiella* growth. **(A, B)** NT, Rab11a, or Rab35 siRNA-transfected cells were infected with mCherry-*Coxiella* and subjected to a second round of siRNA transfection. At the indicated time points, cells were fixed and subjected to immunofluorescent assay with anti-LAMP1 antibody to label the CCVs. Mounted cells were visualized with a Leica Stellaris confocal microscope and analyzed in ImageJ FIJI. measurement of the CCV area revealed significantly smaller CCVs in siRab11a-transfected cells at 3 dpi and siRab35-transfected cells at 6 dpi. Data shown as mean ± SEM of at least 25 cells per condition in each of three independent experiments (N=3) as analyzed by Welch's t-test. **(C)** Colony forming unit assay revealed a significant reduction in *Coxiella* intracellular growth in Rab knockdown cells at both 3 and 6 dpi compared to NT control. Data shown as mean ± SEM of two independent experiments with two biological replicates and three technical replicates each. *, P<0.05; **, P<0.01; ****, P<0.0001.

TABLE 2 Percent reductions in fold change in *Coxiella* intracellular growth over 0 dpi compared to NT control.

Conditions	Percent reduction in fold change	
	3 dpi	6 dpi
Rab11a knockdown	52.6% (p=0.0269)	44.9% (p=0.0192)
Rab35 knockdown	60.8% (p=0.0181)	60.4% (p=0.0083)

p values in parentheses indicate statistical differences between NT control and the respective conditions.

observation that *Coxiella* expands the endosomal compartment in infected host cells (Larson and Heinzen, 2017). It is possible that an increased number of recycling endosomes accumulated more Tf488 in *Coxiella*-infected cells observed in that study (Larson and Heinzen, 2017). Interestingly, in our study, we did not observe an increase in the recycling endosome content at 6 dpi. This may be a result of an already low number of endosomes in the *Coxiella*-infected cells at 6 dpi (Samanta et al., 2019). Nonetheless, these data, taken together with our previous data indicate that *Coxiella* has a dual effect on host endosomes: while it reduces the number of mature endosomes in infected cells (Samanta et al., 2019), *Coxiella*

simultaneously elevates the number of recycling endosomes during infection. While the full characterization of these regulations requires further testing, we propose a model that *Coxiella* reroutes the 'immature' endosomes from the degradative pathway into the recycling pathway, potentially protecting the host cell from the detriments of the 'immature' endosomes.

Finally, our siRNA-mediated knockdown experiments revealed that Rab11a and Rab35 are essential for CCV expansion at 3 and 6 dpi, respectively and both Rab11a and Rab35 knockdown resulted in significantly reduced *Coxiella* intracellular growth. A recent study with Rab11a knockout HeLa cells revealed that Rab11a deficiency increases the number of late endosomes and lysosomes within the cells (Zulkefli et al., 2019). It is possible that in our experiments, Rab11a knockdown led to an increased number of lysosomes which is detrimental to CCV acidity and *Coxiella* growth. Future research analyzing the lysosomal pH and enzyme activity in *Coxiella*-infected, Rab11a/Rab35 knockdown cells will help further characterize the CCV-recycling endosome interactions.

Overall, our data revealed novel host-*Coxiella* interactions that appear to be beneficial for CCV maturation. Future research into characterizing the role of Rab11a and Rab35 in *Coxiella* pathogenesis, and the molecular mechanisms of *Coxiella* enhancement of recycling endosome content will potentially identify novel therapeutic targets for *Coxiella*.

Data availability statement

The raw data supporting the conclusions of this article will be made available by the authors, without undue reservation.

Author contributions

BH: Data curation, Formal analysis, Investigation, Methodology, Software, Writing – original draft, Writing – review & editing. KS: Data curation, Investigation, Methodology, Writing – review & editing. NO: Data curation, Investigation, Methodology, Writing – review & editing. DS: Conceptualization, Data curation, Formal analysis, Funding acquisition, Investigation, Methodology, Project administration, Resources, Software, Supervision, Validation, Visualization, Writing – original draft, Writing – review & editing.

Conflict of interest

The authors declare that the research was conducted in the absence of any commercial or financial relationships that could be construed as a potential conflict of interest.

Publisher's note

All claims expressed in this article are solely those of the authors and do not necessarily represent those of their affiliated organizations, or those of the publisher, the editors and the reviewers. Any product that may be evaluated in this article, or claim that may be made by its manufacturer, is not guaranteed or endorsed by the publisher.

References

Allgood, S. C., Duenas Romero, B. P., Noll, R. R., Pike, C., Lein, S., and Neunuebel, M. R. (2017). *Legionella* effector ankX disrupts host cell endocytic recycling in a phosphocholination-dependent manner. *Front. Cell Infect. Microbiol.* 7, 397. doi: 10.3389/fcimb.2017.00397

Allgood, S. C., and Neunuebel, M. R. (2018). The recycling endosome and bacterial pathogens. *Cell Microbiol.* 20, e12857. doi: 10.1111/cmi.v20.7

Alonso, E., Lopez-Etxaniz, I., Hurtado, A., Liendo, P., Urbaneja, F., Aspiritxaga, I., et al. (2015). Q Fever Outbreak among Workers at a Waste-Sorting Plant. *PloS One* 10 (9), e0138817. doi: 10.1371/journal.pone.0138817

Amitai, Z., Bromberg, M., Bernstein, M., Raveh, D., Keysary, A., David, D., et al. (2010). A large Q fever outbreak in an urban school in central Israel. *Clin. Infect. Dis.* 50 (11), 1433–1438. doi: 10.1086/652442

Angelakis, E., Mediannikov, O., Socolovschi, C., Mouffok, N., Bassene, H., Tall, A., et al. (2014). *Coxiella burnetii*-positive PCR in febrile patients in rural and urban Africa. *Int. J. Infect. Dis.* 28, 107–110. doi: 10.1016/j.ijid.2014.05.029

Baetz, N. W., and Goldenring, J. R. (2013). Rab11-family interacting proteins define spatially and temporally distinct regions within the dynamic Rab11a-dependent recycling system. *Mol. Biol. Cell* 24, 643–658. doi: 10.1091/mbc.e12-09-0659

Beare, P. A., Howe, D., Cockrell, D. C., Omsland, A., Hansen, B., and Heinzen, R. A. (2009). Characterization of a *Coxiella burnetii* ftsZ mutant generated by Himar1 transposon mutagenesis. *J. Bacteriol* 191 (5), 1369–1381. doi: 10.1128/JB.01580-08

Beron, W., Gutierrez, M. G., Rabinovitch, M., and Colombo, M. I. (2002). *Coxiella burnetii* localizes in a Rab7-labeled compartment with autophagic characteristics. *Infect. Immun.* 70 (10), 5816–5821. doi: 10.1128/IAI.70.10.5816-5821.2002

Bjork, A., Marsden-Haug, N., Nett, R. J., Kersh, G. J., Nicholson, W., Gibson, D., et al. (2014). First reported multistate human Q fever outbreak in the United States, 2011. *Vector Borne Zoonotic Dis.* 14 (2), 111–117. doi: 10.1089/vbz.2012.1202

Chaineau, M., Ioannou, M. S., and McPherson, P. S. (2013). Rab35: GEFs, GAPs and effectors. *Traffic* 14, 1109–1117. doi: 10.1111/tra.12096

Chavrier, P., Parton, R. G., Hauri, H. P., Simons, K., and Zerial, M. (1990). Localization of low molecular weight GTP binding proteins to exocytic and endocytic compartments. *Cell* 62 (2), 317–329. doi: 10.1016/0092-8674(90)90369-P

Clemens, D. L., and Horwitz, M. A. (1995). Characterization of the *Mycobacterium tuberculosis* phagosome and evidence that phagosomal maturation is inhibited. *J. Exp. Med.* 181, 257–270. doi: 10.1084/jem.181.1.257

Coleman, S. A., Fischer, E. R., Howe, D., Mead, D. J., and Heinzen, R. A. (2004). Temporal analysis of *Coxiella burnetii* morphological differentiation. *J. Bacteriol* 186 (21), 7344–7352. doi: 10.1128/JB.186.21.7344-7352.2004

Connor, M. G., Pulsifer, A. R., Price, C. T., Abu Kwaik, Y., and Lawrenz, M. B. (2015). *Yersinia pestis* requires host rab1b for survival in macrophages. *PloS Pathog.* 11 (10), e1005241. doi: 10.1371/journal.ppat.1005241

Dejgaard, S. Y., Murshid, A., Erman, A., Kizilay, O., Verbich, D., Lodge, R., et al. (2008). Rab18 and Rab43 have key roles in ER-Golgi trafficking. *J. Cell Sci.* 121, 2768–2781. doi: 10.1242/jcs.021808

Dragan, A. L., Kurten, R. C., and Voth, D. E. (2019). Characterization of early stages of human alveolar infection by the Q fever agent *Coxiella burnetii*. *Infect. Immun.* 87 (5):e00028–19. doi: 10.1128/IAI.00028-19

Eldin, C., Mahamat, A., Demar, M., Abboud, P., Djossou, F., and Raoult, D. (2014). Q fever in French Guiana. *Am. J. Trop. Med. Hyg* 91 (4), 771–776. doi: 10.4269/ajtmh.14-0282

Faris, R., Merling, M., Andersen, S. E., Dooley, C. A., Hackstadt, T., and Weber, M. M.. (2019). *Chlamydia trachomatis* CT229 subverts rab GTPase-dependent CCV trafficking pathways to promote chlamydial infection. *Cell Rep.* 26 (12), 3380–3390.e5. doi: 10.1016/j.celrep.2019.02.079

Ghigo, E., Colombo, M. I., and Heinzen, R. A. (2012). The *Coxiella burnetii* parasitophorous vacuole. *Adv. Exp. Med. Biol.* 984, 141–169. doi: 10.1007/978-94-007-4315-1_8

Goud, B., Zahraoui, A., Tavitian, A., and Saraste, J. (1990). Small GTP-binding protein associated with Golgi cisternae. *Nature* 345 (6275), 553–556. doi: 10.1038/345553a0

Graham, J. G., Winchell, C. G., Kurten, R. C., and Voth, D. E. (2016). Development of an ex vivo tissue platform to study the human lung response to *Coxiella burnetii*. *Infect. Immun.* 84 (5), 1438–1445. doi: 10.1128/IAI.00012-16

Grant, B. D., and Donaldson, J. G. (2009). Pathways and mechanisms of endocytic recycling. *Nat. Rev. Mol. Cell Biol.* 10, 597–608. doi: 10.1038/nrm2755

Green, E. G., Ramm, E. N., Riley, M., Spiro, D. J., Goldenring, J. R., Wessling-Resnick, M., et al. (1997). Rab11 is associated with transferrin-containing recycling compartments in K562 cells. *Biochem. Biophys. Res. Commun.* 239 (2), 612–616. doi: 10.1006/bbrc.1997.7520

Hopkins, C. R., and Trowbridge, I. S. (1983). Internalization and processing of transferrin and the transferrin receptor in human carcinoma A431 cells. *J. Cell Biol.* 97, 508–521. doi: 10.1083/jcb.97.2.508

Horwitz, M. A. (1983). The Legionnaires' disease bacterium (*Legionella pneumophila*) inhibits phagosome-lysosome fusion in human monocytes. *J. Exp. Med.* 158, 2108–2126. doi: 10.1084/jem.158.6.2108

Howe, D., Melnicakova, J., Barak, I., and Heinzen, R. A. (2003). Maturation of the *Coxiella burnetii* parasitophorous vacuole requires bacterial protein synthesis but not replication. *Cell Microbiol.* 5 (7), 469–480. doi: 10.1046/j.1462-5822.2003.00293.x

Howe, D., and Mallavia, L. P. (2000). *Coxiella burnetii* exhibits morphological change and delays phagolysosomal fusion after internalization by J774A.1 cells. *Infect. Immun.* 68, 3815–3821. doi: 10.1128/IAI.68.7.3815-3821.2000

Huang, B., Hubber, A., McDonough, J. A., Roy, C. R., Scidmore, M. A., Carlyon, J. A., et al. (2010). The *Anaplasma phagocytophilum*-occupied vacuole selectively recruits Rab-GTPases that are predominantly associated with recycling endosomes. *Cell Microbiol.* 12, 1292–1307. doi: 10.1111/j.1462-5822.2010.01468.x

Huber, L. A., Pimplikar, S., Parton, R. G., Virta, H., Zerial, M., Simons, K., et al. (1993). Rab8, a small GTPase involved in vesicular traffic between the TGN and the basolateral plasma membrane. *J. Cell Biol.* 123, 35–45. doi: 10.1083/jcb.123.1.35

Huotari, J., and Helenius, A. (2011). Endosome maturation. *EMBO J.* 30, 3481–3500. doi: 10.1038/emboj.2011.286

Junutula, J. R., Maziere De, A. M., Peden, A. A., Ervin, K. E., Advani, R. J., van Dijk, S. M., et al. (2004). Rab14 is involved in membrane trafficking between the Golgi complex and endosomes. *Mol. Biol. Cell* 15 (5), 2218–2229. doi: 10.1091/mbc.e03-10-0777

Kohler, L. J., Reed Sh, C., Sarraf, S. A., Arteaga, D. D., Newton, H. J., and Roy, C. R. (2016). Effector protein cig2 decreases host tolerance of infection by directing constitutive fusion of autophagosomes with the *Coxiella*-containing vacuole. *MBio* 7 (4):e01127–16. doi: 10.1128/mBio.01127-16

Kouranti, I., Sachse, M., Arouche, N., Goud, B., and Echard, A. (2006). Rab35 regulates an endocytic recycling pathway essential for the terminal steps of cytokinesis. *Curr. Biol.* 16, 1719–1725. doi: 10.1016/j.cub.2006.07.020

Larson, C. L., and Heinzen, R. A. (2017). High-Content Imaging Reveals Expansion of the Endosomal Compartment during *Coxiella burnetii* Parasitophorous Vacuole Maturation. *Front. Cell Infect. Microbiol.* 7, 48. doi: 10.3389/fcimb.2017.00048

Leiva, N., Capmany, A., and Damiani, M. T. (2013). Rab11-family of interacting protein 2 associates with chlamydial inclusions through its Rab-binding domain and promotes bacterial multiplication. *Cell Microbiol.* 15, 114–129. doi: 10.1111/cmi.12035

Lyytikainen, O., Ziese, T., Schwartlander, B., Matzdorff, P., Kuhnhen, C., Jager, C., et al. (1998). An outbreak of sheep-associated Q fever in a rural community in Germany. *Eur. J. Epidemiol.* 14 (2), 193–199. doi: 10.1023/a:1007452503863

Magunda, F., Thompson, C. W., Schneider, D. A., and Noh, S. M. (2016). *Anaplasma marginale* actively modulates vacuolar maturation during intracellular infection of its tick vector, *Dermacentor andersoni*. *Appl. Environ. Microbiol.* 82, 4715–4731. doi: 10.1128/AEM.01030-16

Maurin, M., and Raoult, D. (1999). Q fever. *Clin. Microbiol. Rev.* 12, 518–553. doi: 10.1128/CMR.12.4.518

Molleken, K., and Hegemann, J. H. (2017). Acquisition of Rab11 and Rab11-Fip2-A novel strategy for *Chlamydia pneumoniae* early survival. *PloS Pathog.* 13 (8), e1006556. doi: 10.1371/journal.ppat.1006556

Mulye, M., Samanta, D., Winfree, S., Heinzen, R. A., and Gilk, S. D. (2017). Elevated cholesterol in the *Coxiella burnetii* intracellular niche is bacteriolytic. *mBio* 8(1): e02313–16. doi: 10.1128/mBio.02313-16

Nett, R. J., Helgerson, S. D., and Anderson, A. D. (2013). Clinician assessment for *Coxiella burnetii* infection in hospitalized patients with potentially compatible illnesses during Q fever outbreaks and following a health alert, Montana, 2011. *Vector Borne Zoonotic Dis.* 13, 128–130. doi: 10.1089/vbz.2012.1007

Newton, H. J., McDonough, J. A., and Roy, C. R. (2013). Effector protein translocation by the *Coxiella burnetii* Dot/Icm type IV secretion system requires endocytic maturation of the pathogen-occupied vacuole. *PloS One* 8, e54566. doi: 10.1371/journal.pone.0054566

O'Sullivan, M. J., and Lindsay, A. J. (2020). The endosomal recycling pathway-at the crossroads of the cell. *Int. J. Mol. Sci.* 21(17):6074.

Ouellette, S. P., and Carabeo, R. A. (2010). A functional slow recycling pathway of transferrin is required for growth of chlamydia. *Front. Microbiol.* 1, 112. doi: 10.3389/fmicb.2010.00112

Plutner, H., Cox, A. D., Pind, S., Khosravi-Far, R., Bourne, J. R., Schwaninger, R., et al. (1991). Rab1b regulates vesicular transport between the endoplasmic reticulum and successive Golgi compartments. *J. Cell Biol.* 115, 31–43. doi: 10.1083/jcb.115.1.31

Porter, S. R., Czaplicki, G., Mainil, J., Horii, Y., Misawa, N., and Saegerman, C. (2011). Q fever in Japan: an update review. *Vet. Microbiol.* 149, 298–306. doi: 10.1016/j.vetmic.2010.11.017

Rejman Lipinski, A., Heymann, J., Meissner, C., Karlas, A., Brinkmann, V., Meyer, T. F., et al. (2009). Rab6 and Rab11 regulate *Chlamydia trachomatis* development and golgin-84-dependent Golgi fragmentation. *PloS Pathog.* 5 (10), e1000615. doi: 10.1371/journal.ppat.1000615

Ren, M., Xu, G., Zeng, J., De Lemos-Chiarandini, C., Adesnik, M., and Sabatini, D. D. (1998). Hydrolysis of GTP on Rab11 is required for the direct delivery of transferrin from the pericentriolar recycling compartment to the cell surface but not from sorting endosomes. *Proc. Natl. Acad. Sci. U.S.A.* 95, 6187–6192. doi: 10.1073/pnas.95.11.6187

Romano, P. S., Gutierrez, M. G., Beron, W., Rabinovitch, M., and Colombo, M. I. (2007). The autophagic pathway is actively modulated by phase II *Coxiella burnetii* to efficiently replicate in the host cell. *Cell Microbiol.* 9, 891–909. doi: 10.1111/j.1462-5822.2006.00838.x

Ryan, T. A. (2003). Kiss-and-run, fuse-pinch-and-linger, fuse-and-collapse: the life and times of a neurosecretory granule. *Proc. Natl. Acad. Sci. U.S.A.* 100, 2171–2173. doi: 10.1073/pnas.0530260100

Samanta, D., Clemente, T. M., Schuler, B. E., and Gilk, S. D. (2019). *Coxiella burnetii* Type 4B Secretion System-dependent manipulation of endolysosomal maturation is required for bacterial growth. *PloS Pathog.* 15 (12), e1007855. doi: 10.1371/journal.ppat.1007855

Schindelin, J., Arganda-Carreras, I., Frise, E., Kaynig, V., Longair, M., Pietzsch, T., et al. (2012). Fiji: an open-source platform for biological-image analysis. *Nat. Methods* 9, 676–682. doi: 10.1038/nmeth.2019

Siadous, F. A., Cantet, F., Van Schaik, E., Burette, M., Allombert, J., Lakhani, A., et al. (2021). *Coxiella* effector protein CvpF subverts RAB26-dependent autophagy to promote vacuole biogenesis and virulence. *Autophagy* 17, 706–722. doi: 10.1080/15548627.2020.1728098

Ullrich, O., Reinsch, S., Urbe, S., Zerial, M., and Parton, R. G. (1996). Rab11 regulates recycling through the pericentriolar recycling endosome. *J. Cell Biol.* 135, 913–924. doi: 10.1083/jcb.135.4.913

van der Sluijs, P., Hull, M., Webster, P., Male, P., Goud, B., and Mellman, I. (1992). The small GTP-binding protein Rab4 controls an early sorting event on the endocytic pathway. *Cell* 70, 729–740. doi: 10.1016/0092-8674(92)90307-X

Voth, D. E., Howe, D., Beare, P. A., Vogel, J. P., Unsworth, N., Samuel, J. E., et al. (2009). The *Coxiella burnetii* ankyrin repeat domain-containing protein family is heterogeneous, with C-terminal truncations that influence Dot/Icm-mediated secretion. *J. Bacteriol* 191, 4232–4242. doi: 10.1128/JB.01656-08

Voth, D. E., and Heinzen, R. A. (2007). Lounging in a lysosome: the intracellular lifestyle of *Coxiella burnetii*. *Cell Microbiol.* 9, 829–840. doi: 10.1111/j.1462-5822.2007.00901.x

Wandinger-Ness, A., and Zerial, M. (2014). Rab proteins and the compartmentalization of the endosomal system. *Cold Spring Harb. Perspect. Biol.* 6, a022616. doi: 10.1101/cshperspect.a022616

Wang, T., and Hong, W. (2002). Interorganellar regulation of lysosome positioning by the Golgi apparatus through Rab34 interaction with Rab-interacting lysosomal protein. *Mol. Biol. Cell* 13, 4317–4332. doi: 10.1091/mbc.e02-05-0280

White, B., Brooks, T., and Seaton, R. A. (2013). Q fever in military and paramilitary personnel in conflict zones: case report and review. *Travel Med. Infect. Dis.* 11, 134–137. doi: 10.1016/j.tmaid.2012.11.001

Yoshimura, S., Egerer, J., Fuchs, E., and Haas, A. K., and Barr, F. A. (2007). Functional dissection of Rab GTPases involved in primary cilium formation. *J. Cell Biol.* 178 (3), 363–369. doi: 10.1083/jcb.200703047

Zheng, J. Y., Koda, T., Fujiwara, T., Kishi, M., Ikehara, Y., and Kakinuma, M. (1998). A novel Rab GTPase, Rab33B, is ubiquitously expressed and localized to the medial Golgi cisternae. *J. Cell Sci.* 111, 1061–1069. doi: 10.1242/jcs.111.8.1061

Zulkefli, K. L., Houghton, F. J., Gosavi, P., and Gleeson, P. A. (2019). A role for Rab11 in the homeostasis of the endosome-lysosomal pathway. *Exp. Cell Res.* 380, 55–68. doi: 10.1016/j.yexcr.2019.04.010